Clim Dyn (2009) 32:565–574
DOI 10.1007/s00382-008-0453-z

Impact of subgrid scale scheme on topography and landuse for better regional scale simulation of meteorological variables over the western Himalayas

A. P. Dimri

Received: 10 October 2007 / Accepted: 1 August 2008 / Published online: 29 August 2008

Abstract An attempt is made to integrate subgrid scale scheme on the work of Dimri and Ganju (Pure Appl Geophys 167:1–24, 2007) to understand the overall nature of surface heterogeneity and landuse variability along with resolvable finescale micro/meso scale circulation over the Himalayan region, which is having different altitudes and orientations causing prevailing weather conditions to be complex. This region receives large amount of precipitation due to eastward moving low-pressure synoptic weather systems, called western disturbances, during winter season (December, January, February—DJF). Surface heterogeneity and landuse variability of the Himalayan region gives rise to numerous micro/meso scale circulation along with prevailing weather. Therefore, in the present work, a mosaic type parameterization of subgrid scale topography and landuse within a framework of a regional climate model (RegCM3) is extended to study interseasonal variability of surface climate during a winter season (October 1999–March 2000) of the work of Dimri and Ganju (Pure Appl Geophys 167:1–24, 2007). In this scheme, meteorological variables are disaggregated from the coarse grid to the fine grid, land surface calculations are then performed separately for each subgrid cell, and surface fluxes are calculated and reaggregated onto the coarse grid cell for input to the atmospheric model. By doing so, resolvable finescale structures due to surface heterogeneity and landuse variability at coarse grid are subjected to parameterize at regular finescale surface subgrid. Model simulations show that implementation of subgrid scheme presents more realistic simulation of precipitation and surface air temperature. Influence of topographic elevation and valleys is better represented in the scheme. Overall, RegCM3 with subgrid scheme provides more accurate representation of resolvable finescale atmospheric/surface circulations that results in explaining mean variability in a better way.

Keywords Regional climate · Climate variability · Western Himalayas

A. P. Dimri (✉)
School of Environmental Sciences, Jawaharlal Nehru University, New Delhi 110067, India
e-mail: apdimri@hotmail.com; apdimri@yahoo.com

1 Introduction

In the Indian part of the western Himalayas surface weather elements, like precipitation and temperature, are intensely governed by local topography (Dimri 2004) and local atmospheric circulations (Mohanty and Dimri 2004). Landuse variability and topographic heterogeneity gives rise to numerous micro/meso scale circulation from surface level energy and mass exchanges (Dickinson 1995; Pielke and Avissar 1990). In addition, different altitude and orientation of the Himalayan ranges give rise to different thermodynamical and dynamical forcing. These factors modulate the western disturbances (WDs) embedded in the zonal westerlies up to great extent and hence determine precipitation and temperature pattern over the region (Dimri and Mohanty 1999).

Regional climate models (RCMs) are useful tools for studying mesoscale climatic processes on regional scale. Giorgi et al. (1993a), Hirakuchi and Giorgi (1995), Marinucci and Giorgi (1992) and Jones et al. (1995) have shown that RCMs have worked well over various domains over the globe. Over Indian region, various researchers have carried out regional climate simulation to study monsoon behavior over Indian region. Bhaskaran et al. (1996) has compared seasonal simulation of Indian

Summer Monsoon with a set of three RCMs, which shows the strong orographically forced mesoscale component. Although, various researchers carried out number of studies over the Indian region but they were mainly pertaining with summertime monsoon phenomena and very few studies on multilayer integrations/simulation with RCMs during winter season (DJF) over complex Himalayan region are reported.

In the present study, Dimri and Ganju's (2007) work is extended with an integration of subgrid parameterization scheme with in The Abdus Salam International Center for Theoretical Physics (ICTP)–RegCM3 model. The National Center for Environmental Prediction, US, (NCEP) reanalysis is used as the model boundary conditions. Model simulation is made for 6 months (October 1999–March 2000) to assess mean climate conditions and interseasonal variability and impact of the subgrid parameterization scheme in the model results. In Sect. 2, a brief description of model and experimental design is presented. The results are discussed in Sect. 3 and final remarks are given in Sect. 4.

2 Model and experimental design

The RCM used in the present work is the version of RegCM developed by Giorgi et al. (1993a, b) with some of the updates discussed in Giorgi and Shields (1999). The dynamical core of the RegCM is equivalent to the hydrostatic version of the fifth-generation Pennsylvania State University–National Center for Atmospheric Research (NCAR), US, mesoscale model (MM5). For the present simulation, the standard model configuration is used with 23 sigma levels, with medium resolution PBL scheme with five levels in the lowest 1.5 km of the atmosphere, at approximately 40, 110, 310, 730 and 1,400 m above surface (Giorgi and Bates 1989). The physics parameterization employed in the simulations include the radiative transfer package of the NCAR Community Climate Model version 3 (CCM3, Kiehl et al. 1996), the nonlocal boundary scheme by Holtslag et al. (1999) and mass flux cumulus cloud scheme of Grell (1993). Land surface processes are described via Biosphere-Atmosphere Transfer Scheme or BATS (Dickinson et al. 1993).

Parameterization of land surface heterogeneity—where this term refers to both topography and landuse—can generally be divided into discrete or "mosaic" methods or continuous, or probability density function (pdf), methods. In the mosaic approach, the model grid cell is divided into a number of subgrid cells or tiles, land surface calculations are carried out separately for each tile and the land–atmosphere exchanges are then reaggregated at the original coarse grid cell scale. Subgrid cells have been based on landuse type class (Avissar and Pielke 1989; Koster and Surez 1992), topographic elevation class (Leung and Ghan 1995), or local landuse or topography (Seth et al. 1994). In pdf methods, the heterogeneous variables are represented via analytical or empirical pdfs and relevant processes are integrated over the appropriate pdf (Enthekhabhi and Eagleson 1989; Avissar 1991, 1992; Famiglietti and Wood 1994a, b; Sivapalan and Woods 1995; Dumenil and Todini 1992; Giorgi 1997a, b). Regardless of methods used, all the paper cited earlier clearly show that the subgrid scale heterogeneity in topography and landuse conditions can profoundly affect climate and the surface energy and water budgets, especially at the regional and local scales. It is therefore important to include a representation of land surface heterogeneity within the climate models. Therefore, here implementation of an augmented version of the mosaic type scheme of Seth et al. (1994) within the framework of RCM is attempted. This scheme assumes that each model grid cell is subdivided into a regular subgrid of N cells for which independent land surface calculations are carried out. In particular, the scheme allows a flexible choice of subgrid based on local landuse and topographical information.

In this paper, we compare two simulations: a control run in which the subgrid scheme is not used and therefore the land surface has the same resolution as the atmosphere and a run in which each coarse grid cell is divided into 36 subgrid cells (EXP10). The domain, topography, and landuse distribution used in this control run are shown in Fig. 1a, b. The full domain of the simulations covers most of the area from Mediterranean Sea to India using a Lambert conformal projection with grid cells of 60 km × 60 km size in the control run. Therefore, the land surface grid cell size in the EXP10 experiment is 10 km × 10 km as 60 km × 60 km grid size is divided into 10 km × 10 km subgrid size to incorporate subgrid scale effects into the model. This disaggregation, say for temperature field, is done according to the subgrid elevation difference and can be expressed as

$$T_{i,j}^{\mathrm{sg}} = \overline{T} + \Gamma_T\left(\overline{h} - h_{i,j}^{\mathrm{sg}}\right)$$

where sg is subgrid, i, j is subgrid cell, overbar coarse grid temperature near surface air temperature, h is topographical elevation and Γ_T is average atmospheric lapse rate. Note that as a standard procedure the model topography field receives some additional smoothening in order to remove the shortest wavelengths, so that the effective resolution of the topography field is somewhat coarser than the grid cell size. Here we focus on an area of complex topography and landuse encompassing the Indian Himalayan region and immediately surrounding areas. As an example of the added resolution in the EXP10, Fig. 1c, d

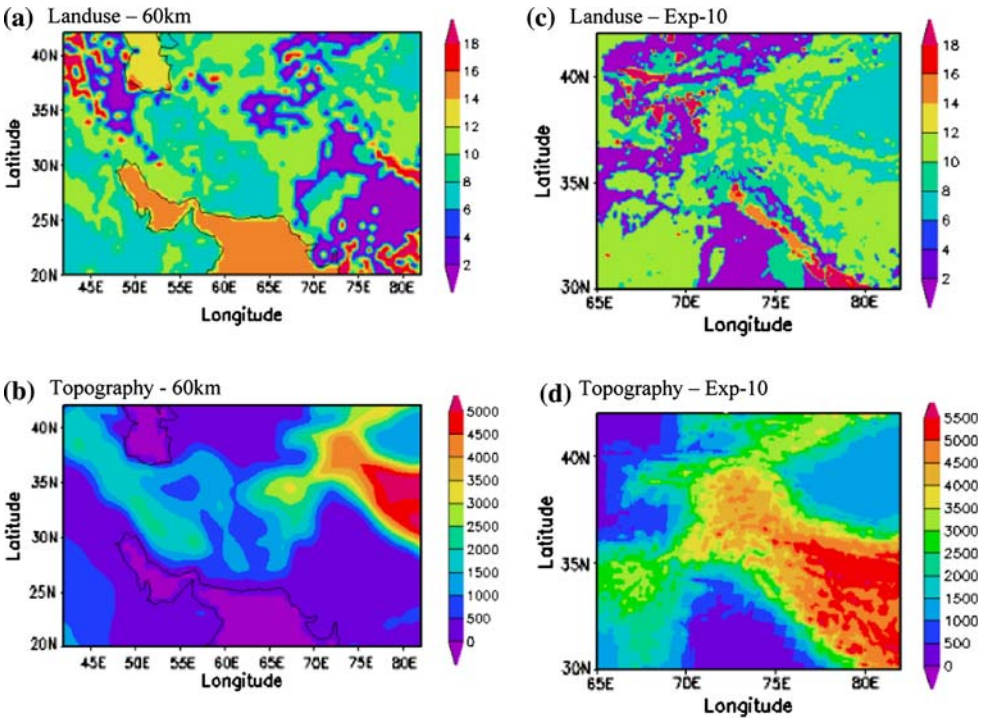

Fig. 1 Landuse and topography over a region encompassing the himalayas **a** landuse, **b** topography in the control run, **c** landuse, Exp-10 and **d** topography, Exp-10. Unit for topography is in meter

shows the topography and landuse distribution over the region of interest. It is evident that at the higher resolution topography of the Indian Himalayan region is described in detail. In addition, substantial subgrid scale variability of vegetation cover is found across the Indian Himalayas in correspondence with the topographic variability.

The topography for control and EXP10 grids is obtained from a 30″ (about 1 km) resolution global datasets produced by the U.S. Geological Survey (USGS). The landuse distribution for the control and EXP10 is also obtained from 30″ landuse dataset produced by USGS (Loveland et al. 1991). A version of this datasets is already available in the form of BATS surface types. From the 30″ dataset, we calculate fractional cover of different surface types for each cell of the different model grids, and the grid cell is then assigned the surface type with the largest fractional cover.

The simulation cover for the 6-month period starting from 1 October 1999, and ending on 31 March 2000, that it encompasses full winter season. This particular period is chosen for the study, as enormous amount of precipitation in the form of snow was received/recorded over Indian part of the western Himalayas. Lateral meteorological boundary conditions for the simulations are obtained from analyses of observations by the NCEP (Kalnay et al. 1996) and therefore the model results can be directly compared with the observations for the simulated period. Soil temperatures are initialized with the temperature of the bottom model level and soil water content is initialized as a function of vegetation type (Giorgi and Bates 1989).

In the present study, the analysis focuses on surface climate variables (temperature, precipitation and snow amount) only. Observed monthly and seasonal precipitation and surface air temperature needed for the evaluation of the simulations are obtained from 0.5° resolution global land datasets developed by the Climate Research Unit (CRU) of the University of East Anglia (New et al. 2000), Willmott and Matuura (2001)—WM and station data from the Snow and Avalanche Study Establishment (SASE), Chandigarh, India.

3 Results

In this section, overall evaluation of the model performance is provided. Further, the largest effects of subgrid land surface parameterization can be expected in areas of complex topography and landuse. Therefore, a detailed analysis and inter comparison of the different model simulation over the western Himalayas, where surface heterogeneity is maximum, is presented. Results are discussed on monthly and seasonal average variability of surface air temperature, precipitation and snowfall amount. A detailed analysis and comparison of simulations with observation over the Himalayan region are presented. In addition to this, comparison is drawn at three stations, viz., D-10 (latitude 33°31′17″, longitude 75°12′02″, altitude 3,250 m), Bahang (latitude 32°16′33″, longitude 77°09′03″, altitude 2,192 m) and Drass (latitude 34°04′00″, longitude 75°08′00″, altitude 3,250 m), situated in Indian Himalayan region. These

stations are chosen in such a way that they represent different climatic and geographic conditions of the region and have recorded data. Also, statistics and associated error analysis, in terms of root mean square error (RMSE) and correlation coefficient (CC), is carried out to assess model's skill.

3.1 Surface air temperature

Figure 2a–c compares seasonal (October 1999–March 2000) average observed temperature (CRU) and simulated surface air temperature in control and subgrid experiment over the region shown in Fig. 1, which includes our focus over the Himalayan region of complex topographical features. In winter, Fig. 2b, the seasonal temperature patterns are reproduced with reasonable satisfaction over the Himalayan region in control run. Also, control simulation shows less detail temperature distribution pattern than the observation in particular over the main mountainous ranges. Some of this may be attributed to the fact that observational data is an integration of multiple types/sources of data and control simulation results are affected by smoothening of model topography. Whereas, effect of subgrid scale heterogeneity shows pronounced temperature variability due to surface subgrid parameterization over the region, Fig. 2c. The observations do not show finescale structure as here subgrid parameterization scheme enhances the initial landuse information in the model simulation. In control run lower temperature values, say less than -17°C, are not captured well as compared to the higher surface resolution run. This is important because areas of minimum temperature not only occur over the Himalayan region but also comprise number of valleys and hills. This is due to the topographic correction of the temperature field employed in the disaggregation scheme. Note that areas of lowest temperature than in the control run are found in subgrid scheme simulation within the Himalayan region. Zone of negative temperatures are in corroboration with the fact that finer resolvable scale circulations are well depicted in the subgrid scale scheme. These occur in correspondence with the topography resolved in the finer resolution. Figures indicate that the subgrid surface scheme leads to increased spatial details of temperature and that the simulated temperature is in better agreement with observations. It is seen that subgrid scale simulations, Fig. 2c, could able to capture more information of extreme cold temperature distribution over the region. Also, spatial distribution of cold temperature is more enhanced in subgrid scale simulation than the control run. Control run could not reproduce the finescale temperature distribution. This could be due to the fact that heterogeneity in topography and landuse is complex to represent in the model with finer scale. Figure 2d represents monthly averaged observed and simulated surface air temperature at three of the stations located in the western Himalayas. Temperature values of the grid in which these stations fall are considered from CRU, WM and simulated experiments for comparison. It shows large variation in monthly averaged surface air temperature at any station over the region. However, model simulations could produce negative temperature distribution as shown by the station data than the observed (CRU and WM). It could be attributed to the fact that finer details of heterogeneity in topography and landuse are represented in the model with finer scale. Whereas, in observations, CRU and WM, representation of density of high and low elevation stations may not be that homogeneous so that fine resolution resolvable scale circulations are not reproduced. Further, comparison, Fig. 2e, shows that model has tendency to overestimate the cold region temperatures and underestimate the warm region temperatures by few degrees. Over the complex mountainous region model shows warm bias by few degrees. It is likely that the model bias is artificially enhanced by a temperature overestimates in the observed dataset induced by the relatively low density of high elevation stations. Also, Fig. 2f represents model's skill in terms of RMSE and CC associated with CRU and control run experiment along with area averaged temperature anomaly during model simulation period. Skill, RMSE $= 0.34$ and CC $= 0.99$, shows that model simulation could follow temperature trend as per the observation. In addition to this, monthly temperature variability in terms of temperature anomaly is well captured by the model simulation. Temperature anomaly distribution explicitly explains similar anomaly pattern between the two. Coming back to the resolvable scale simulation using subgrid parameterization scheme (Fig. 2c), it is seen that finer scale distribution of surface air temperature are brought out. The subgrid scheme simulations are able to represent the temperature distribution with much finer details. Due to smoothening of topography in model simulations fine resolution resolvable scale circulations do not get reproduced well (Dimri 2004). It is evident with the fact that in subgrid scheme simulations topographical distribution is well resolved to bring out the finer scale surface circulation over the region which is comprised of valleys and hill ranges. Regions of extreme cold temperature which are not captured in the control run simulation are well produced in subgrid scheme simulation. Effects of topographic heterogeneity in surface air temperature have enhanced model results in subgrid scheme. This highlights the fact that resolvable scale features are better represented in subgrid scheme simulation. Overall, the comparison of the figures indicates that the model could reproduce the observed regional temperature pattern over the Himalayan region.

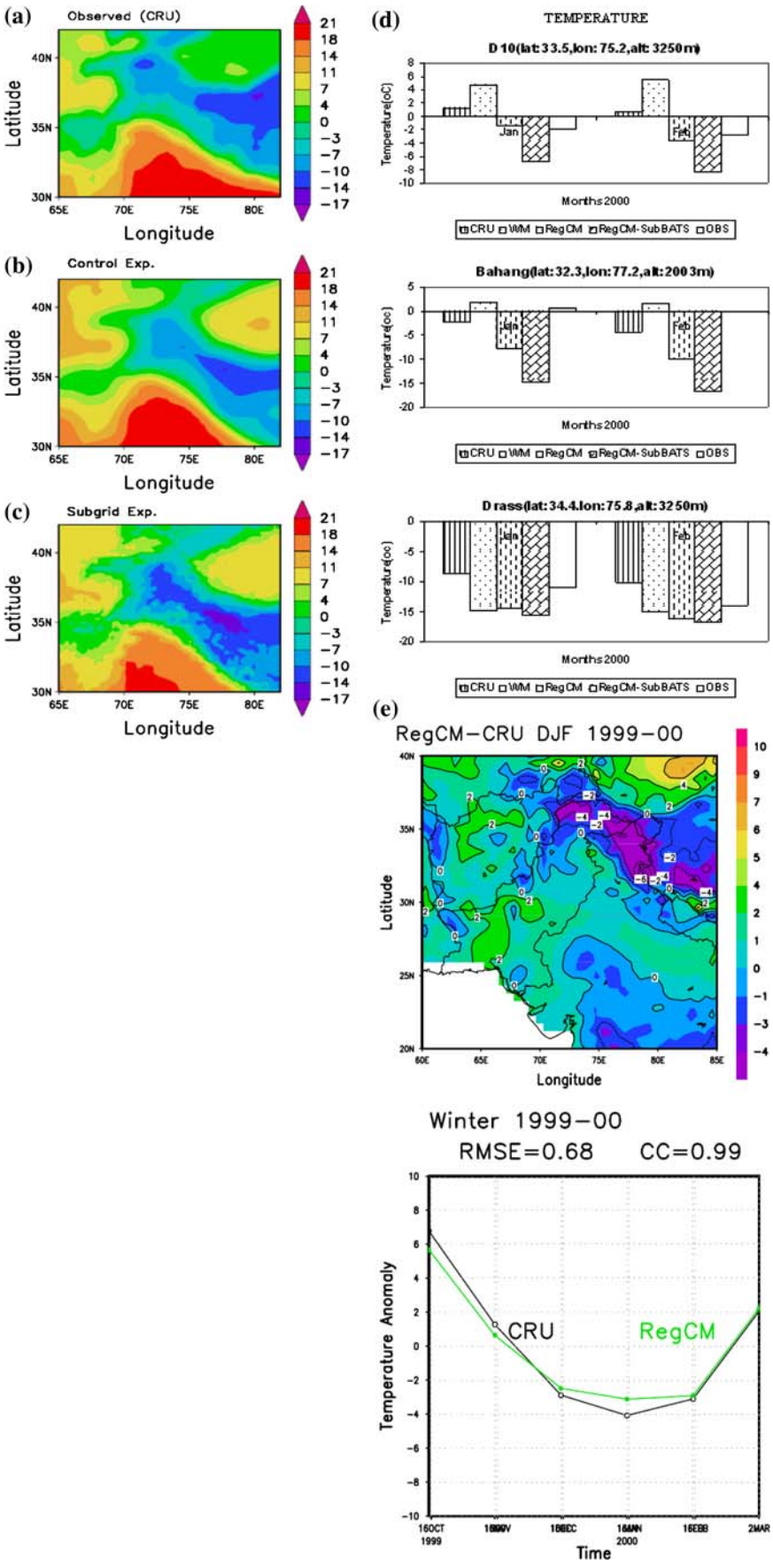

Fig. 2 Observed (CRU) and simulated (control experiment and subgrid experiment) monthly average surface air temperature (°C) over the Himalayan region. **a** Observed, winter; **b** control, winter; and **c** subgrid experiment, winter; **d** station wise comparison; **e** seasonal temperature bias; **f** temperature model statistics

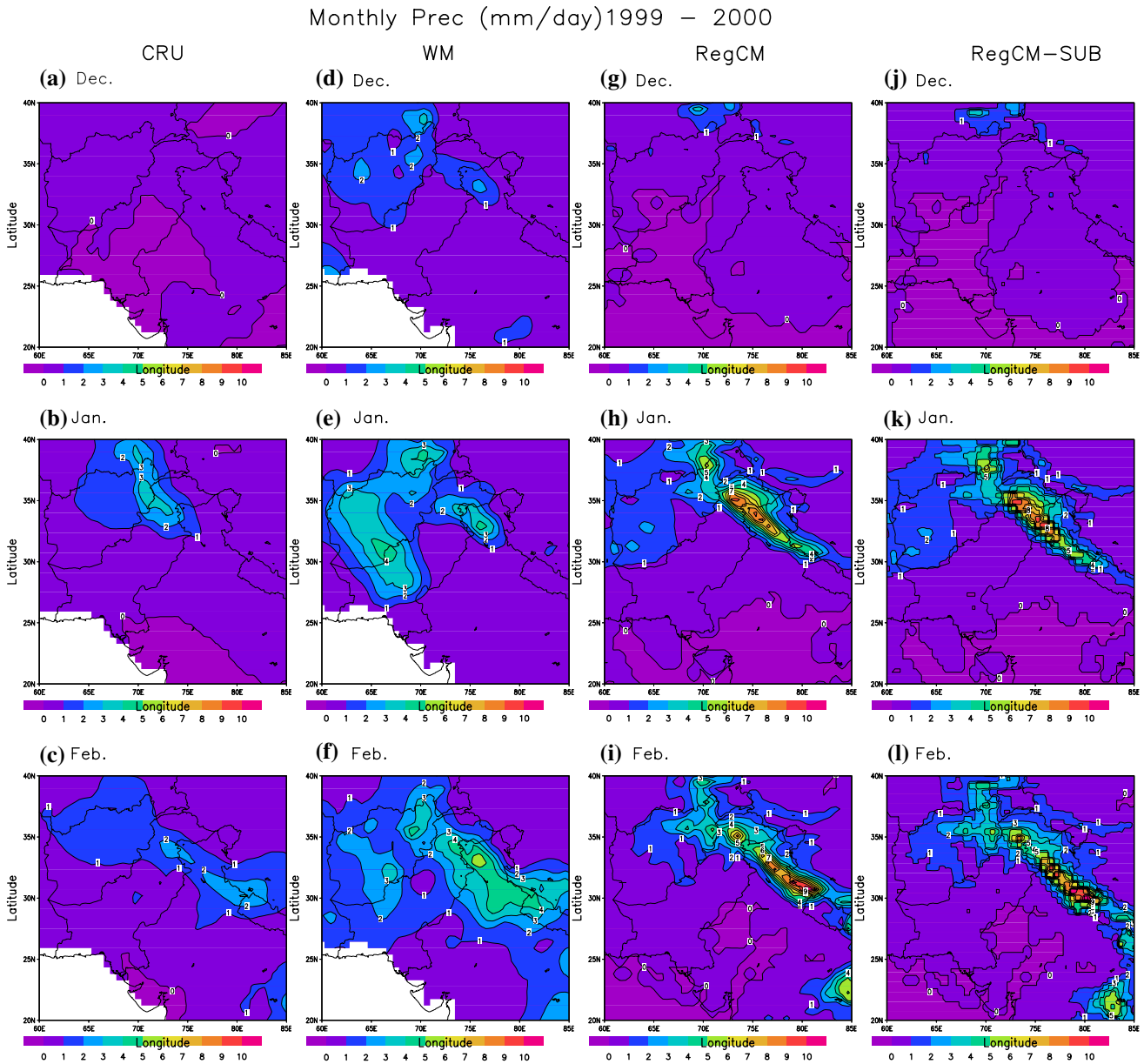

Fig. 3 Observed (CRU and WM) and simulated (control experiment and subgrid experiment) monthly average precipitation (mm/day) for December, January and February over the Himalayan region

3.2 Precipitation

Figure 3 presents the comparison of monthly average precipitation (December, January and February) between two sets of observed (CRU, Fig. 3a–c and WM, Fig. 3d–f) and simulated (control experiment, Fig. 3g–i and subgrid experiment, Fig. 3j–l) precipitation fields. Figures show that model could able to simulate well the variability associated in the nature of precipitation up to certain extent and hence monthly averaged precipitation are simulated well with overestimation in the model nature. Apart from this, subgrid scale experiment (Fig. 3j–l) could reproduce monthly averaged precipitation field better than that due to the control experiment (Fig. 3g–i). Again, it is iterated that, in CRU and WM observations representation of density of high elevation and low elevation stations may not be that homogeneous so that fine resolution resolvable scale circulations are not reproduced. Further, comparison shows that model has a tendency to overestimate the precipitation over the Himalayan region. These biases can be attributed to the facts that due to the relatively low density of high elevation stations in observed data sets.

Further, Fig. 4a–c compares seasonal averaged (October 1999–March 2000) observed (CRU) precipitation and

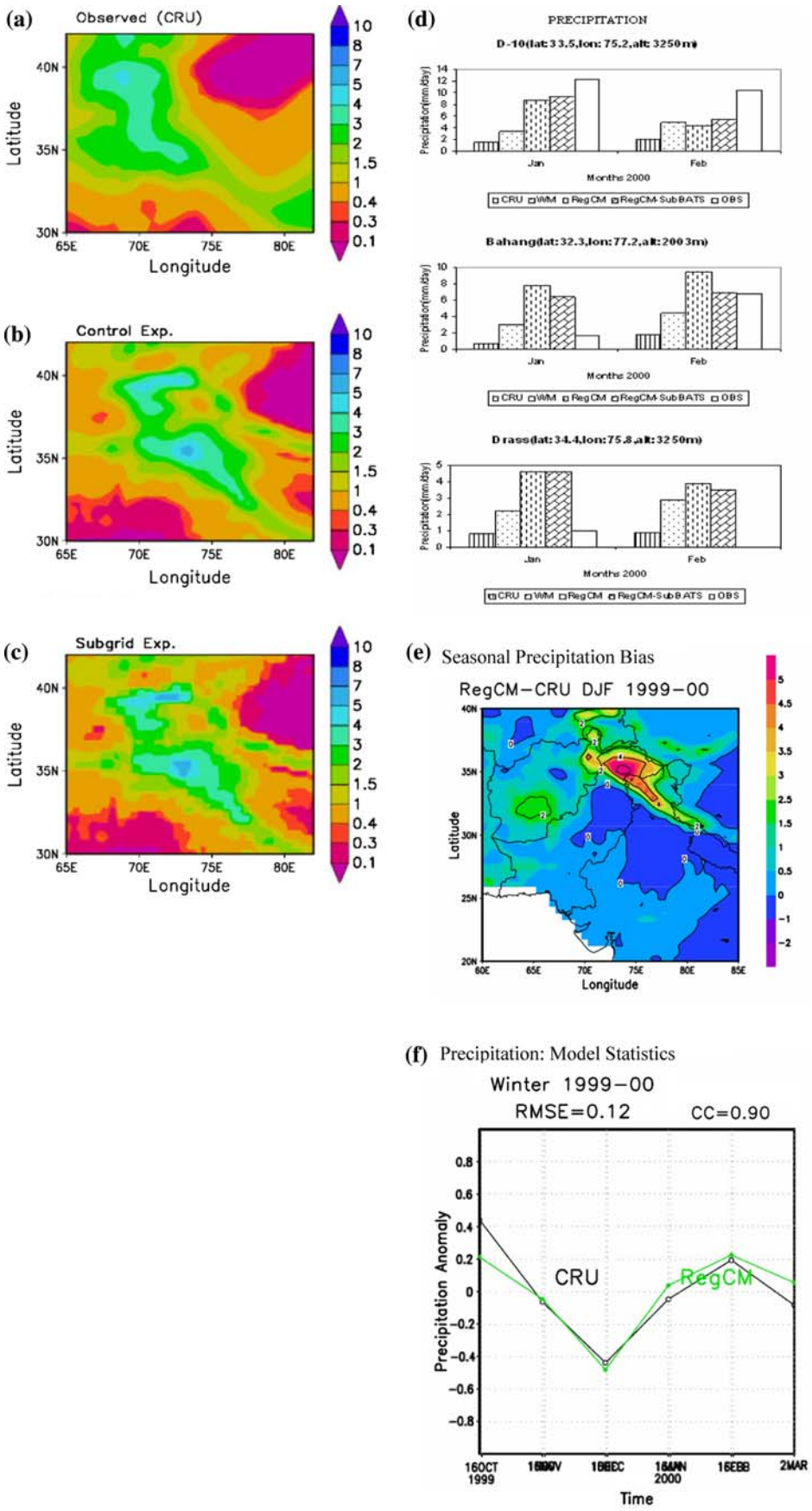

Fig. 4 Same as Fig. 3, but for seasonal average precipitation (mm/day)

simulated experiments (control run and subgrid scale experiment) over the Himalayan region. Though the control experiment could able to reproduce the precipitation distribution pattern but not at all scales. However, it could generate well the precipitation amount over northwest Indian region but over the Himalayan region the precipitation patterns are overestimated. This bias may be attributed to the fact that although in general topographically induced cold season precipitation maxima are reproduced, the corresponding peak precipitation values are somewhat overestimated. This problem could be related to relatively coarse resolution of observed data set CRU; where over the complex topographical Himalayan region station of high elevations are not represented well. Nonetheless, figures indicate that control run simulations are quite close to the actual precipitation amount of 0.1–1.0 mm/day over western Indian region of Gujarat, Rajasthan and Punjab, whereas, over the Indian Himalayan region amount of the precipitation is overestimated by the control run experiment. But based on this, it could be stated that most of the topographically induced precipitation is reproduced well by model simulation, therefore, overall, the model captures regional topographical forcing. The reason of model overestimate is that the dominant precipitation process is mostly of resolvable scale nature and is induced by topographic uplift within eastward moving cyclonic systems (WDs). As a result, precipitation is mostly forced by the topographical gradients and the under representation of these gradients in the model physics leads to over/under estimate of the precipitation maxima. These results are indeed evident from the comparison of the winter precipitation fields in Figs. 3 and 4a, b. Small differences across the simulation are essentially due to the internal model variability (Giorgi and Bi 2000).

In addition to this, Fig. 4c represents the seasonal averaged subgrid scale experiments. Simulation experiment shows high intensity of precipitation maxima, lying along the orientation of the Himalayan region, which are not shown in observed (CRU) datasets as up to certain extent in control experiment also. This difference may lie in the fact that topography and vegetation cover is very fast changing within a kilometer over the Himalayan region where as observed dataset is presented at 0.5° resolution. Further, while comparing simulation experiments it is seen that implementation of subgrid scheme could produce finer details of precipitation distribution well. In addition to this, Fig. 4d illustrates monthly averaged observed and simulated precipitation field at three stations. Comparison shows that model simulations could only yield a certain percentage of actual precipitation recorded at D-10, Bahang and Drass. Since precipitation disaggregation scheme is not implemented in the simulation technique, hence simulations show that model produces more moisture than the observed, Fig. 4e. This overestimation of precipitation can be attributed to the fact that due to smoothening of model topography, micro/meso scale circulations, which are dominant in complex topography of the Himalayas, may be overlooked while simulations procedure. Due to topography smoothening low density of high elevation points is considered in the model. Apart from this, smoothening of topography and landuse in simulation experiments reduced the impact of orographic lifting due to steep gradient in the Himalayan region. Most of the time orographic lifting is the predominant mechanism to modulate the precipitation amount in complex topographical region of the Himalayas. Also, smoothening of landuse type, which is rapidly changing within a kilometer in the Himalayan region may lead to over/under estimate of the precipitation amount. Nonetheless, it is seen that up to certain extent the variability in precipitation amount is captured in model simulation, Fig. 4f. Here, precipitation anomaly in simulated and observed field is seen in accordance to each other. And model could be able to show reasonable skill with RMSE = 0.12 and CC = 0.90. Overall the simulations could capture the precipitation pattern well and their variability is well depicted.

3.3 Snow

A variable that can be expected to be substantially sensitive to the subgrid topographic forcing is snow. BATS assumes that precipitation is in the form of snowfall if the near surface air temperature is lower than 2.2°C and rainfall for higher temperature. As a result, the response of the snow can be highly nonlinear, since snow formation and melting are regulated by the processes that are essentially step function of temperature thresholds. Figure 5 compares the seasonal averaged (October 1999–March 2000) snow depth over the Himalayan region in the simulation for winter season. In this section some important points need to be considered. First, the model calculates the snow depths in term of the liquid water equivalent. To obtain equivalent liquid water depth we scaled the snow depth by a factor of 1/3, which is roughly characteristic of the density of the aging snow (Dickinson et al. 1993). Admittedly a large uncertainty is implicit in this assumption. Second, the station density is irregular in space and it includes a relatively small number of high elevation stations. Third, observed snow depth at a station is strongly affected by processes such as snowdrift and snow sheltering by upwind obstacles, which are not included in the model. For these reasons the snow depth study is necessarily limited in scope and mostly aim at providing qualitative indications of the model behavior.

It is evident from Fig. 5 that the spatial variability of snow increases substantially with the resolution of the land

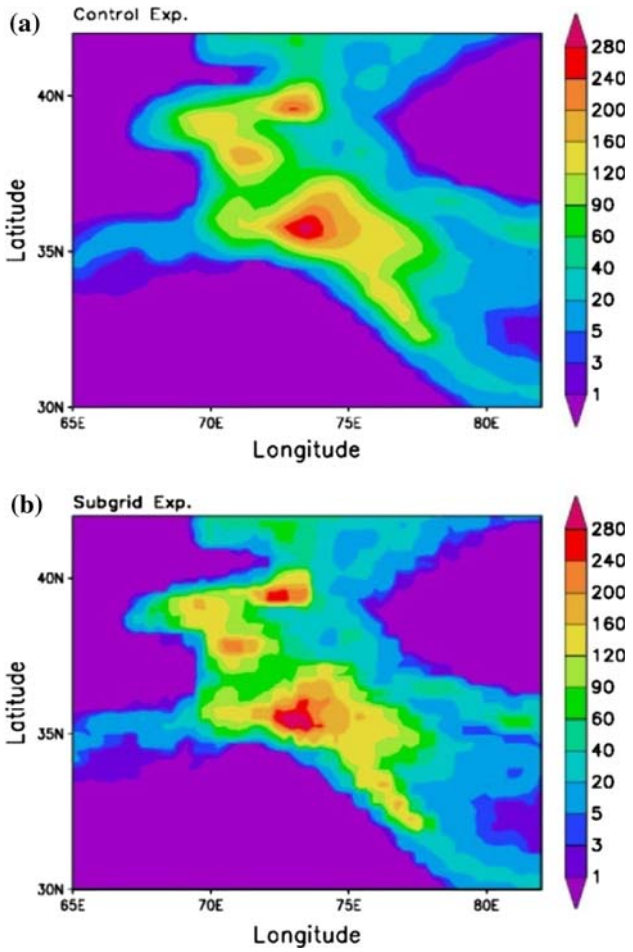

Fig. 5 Simulated seasonal average snow amount (mm/day) over the Himalayan region. **a** Control, winter and **b** subgrid experiment, winter

surface. This is because the temperature disaggregation produced is such that precipitation can be in the form of snowfall over the higher subgrid peaks and rainfall over the subgrid valleys even though the coarse grid precipitation is only in the form of rainfall or snowfall. As a result, snow tends to accumulate over the high resolution peaks and melt more effectively over the corresponding valleys. This can be expected from the complex Himalayan topography illustrated in Fig. 1, and the limited understanding shows that in the subgrid scheme, the spatial scale of snow depth variability is more pronounced. Indeed even with the limitations discussed previously, it clearly shows that snow depth is characterized by a pronounced finescale variability. In winter, not only the spatial variability of snow increases with subgrid resolution, but also do overall snow amounts over the region. This can be attributed to the inherent nonlinear nature of snow forming processes. As the temperature threshold for snow formation reached, say at the high elevation of a subgrid peak, snow starts accumulating. Because snow has a higher albedo than a bare soil or vegetation, the overall surface albedo increases and this causes a decrease in absorption of solar radiation at the surface. This in turn inhibits the solar warming of the surface and thus tends to cool the region and increase the lifetime of the snowpack. These feedback processes can be seen in the overall winter cooling of the Himalayan region in subgrid scheme simulation compared to control run and in the greater overall snow amounts shown by the subgrid experiments.

4 Discussion and conclusions

In the present work, subgrid scale scheme is introduced to the work of Dimri and Ganju (2007) and hence Regional Climate Model (RegCM3) is tested with its effects on the surface climate for a 6-month simulation period over the Himalayan region where both topography and landuse variability are high.

Summarizing the results, the subgrid surface scheme significantly affects the variability of temperature and snow depth, as well as the winter precipitation over the Himalayan region. In most cases these affects are in the direction of a better agreement with observations. Overall analysis presented shows that the model reproduced the basic surface climatology of the simulated period both in its seasonal and spatial features. Also, representation of the subgrid scale scheme has improved impact on the variability of the surface processes.

In future, larger time simulation experiments are planned to understand the variabilities associated with these parameter (Dimri and Giorgi 2008).

Acknowledgments The author acknowledges Prof. F. Giorgi, Dr. X. Bi and Dr. N. Elguindi and The Abdus Salam International Center for Theoretical Physics (ICTP), Trieste, Italy for providing necessary help for the above study. Also, authors acknowledge the National Center for Environmental Prediction (NCEP), US for providing valuable data sets for accomplishing this work. Author expresses his gratitude towards Dr. R. N. Sarwade, Director S.A.S.E., for his help and encouragement for the present work.

References

Avissar R, Pielke RA (1989) A parameterization of heterogeneous land surface for atmospheric numerical models and its impact on regional meteorology. Mon Weather Rev 117:2113–2136. doi: 10.1175/1520-0493(1989)117<2113:APOHLS>2.0.CO;2

Avissar R (1991) A statistical dynamical approach to parameterize subgrid scale land surface heterogeneity in climate models. Surv Geophys 12:155–178. doi:10.1007/BF01903417

Avissar R (1992) Conceptual aspects of a statistical dynamical approach to represent landscape subgrid scale heterogeneity in atmospheric models. J Geophys Res 97:2729–2742

Bhaskaran B, Jones RG, Murphy JM, Noguer M (1996) Simulation of Indian summer monsoon using a nested regional climate model: domain size experiments. Clim Dyn 12:573–587

Dickinson RE (1995) Land atmosphere interaction. Rev Geophys 33(Suppl):917–922. doi:10.1029/95RG00284

Dickinson RE, Henderson-Sellers A, Kennedy PJ (1993). Biosphere-atmosphere transfer scheme (BATS) version 1e as coupled to the NCAR Community Climate Model, NCAR technical note NCAR/TN-387+STR, 72 pp

Dimri AP (2004) Impact of horizontal model resolution and orography on the simulation of a western disturbance and its associated precipitation. Meteorol Appl 11(2):115–127. doi:10.1017/S1350482704001227

Dimri AP, Ganju A (2007) Wintertime seasonal scale simulation over Western Himalaya using RegCM3. Pure Appl Geophys 167:1–24

Dimri AP, Mohanty UC (1999) Snowfall statistics of some SASE field stations in J&K and a case study of western disturbance. Def Sci J 49(5):437–445

Dimri AP, Giorgi F (2008) Regional scale simulation with subgrid scale topography and landuse scheme over Western Himalayas (under preparation)

Dumenil L, Todini E (1992) A rainfall runoff scheme for use in the Hamburg climate model. In: O'Kane JP (ed) Advances in theoretical hydrology: a tribute to James Dooge. European Geophysical Society series in hydrological sciences, vol 1. Elsevier, Amsterdam, pp 129–157

Enthekhabhi D, Eagleson P (1989) Land surface hydrology parameterization for the atmospheric general circulation models including subgrid scale spatial variability. J Clim 2:816–831. doi:10.1175/1520-0442(1989)002<0816:LSHPFA>2.0.CO;2

Famiglietti JS, Wood EF (1994a) Application of multiscale water and energy balance model on a tallgrass prairie. Water Resour Res 30:3079–3093. doi:10.1029/94WR01499

Famiglietti JS, Wood EF (1994b) Multiscale modeling of spatially variable water and energy balance processes. Water Resour Res 30:3061–3078. doi:10.1029/94WR01498

Giorgi F (1997a) An approach for the representation of surface heterogeneity in land surface models, Part I: Theoretical framework. Mon Weather Rev 125:1885–1899. doi:10.1175/1520-0493(1997)125<1885:AAFTRO>2.0.CO;2

Giorgi F (1997b) An approach for the representation of surface heterogeneity in land surface models, Part II: Validation and sensitivity experiments. Mon Weather Rev 125:1900–1919. doi:10.1175/1520-0493(1997)125<1900:AAFTRO>2.0.CO;2

Giorgi F, Shields C (1999) Test of precipitation parameterizations available in the latest version of the NCAR regional climate model (RegCM) over the continental United States. J Geophys Res 104:6353–6375. doi:10.1029/98JD01164

Giorgi F, Bates GT (1989) On the climatological skill of a regional model over complex terrain. Mon Weather Rev 117:2325–2347. doi:10.1175/1520-0493(1989)117<2325:TCSOAR>2.0.CO;2

Giorgi F, Bi X (2000) A study of internal variability of a regional climate model. J Geophys Res 105:29503–29521. doi:10.1029/2000JD900269

Giorgi F, Marinucci MR, Bates GT (1993a) Development of a second generation regional climate model (RegCM2), Part I: Boundary layer and radiative transfer processes. Mon Weather Rev 121:2794–2813. doi:10.1175/1520-0493(1993)121<2794:DOASGR>2.0.CO;2

Giorgi F, Marinucci MR, De Canio G, Bates GT (1993b) Development of a second generation regional climate model (RegCM2), Part II: Convective processes and assimilation of lateral boundary conditions. Mon Weather Rev 121:2814–2832. doi:10.1175/1520-0493(1993)121<2814:DOASGR>2.0.CO;2

Grell GA (1993) Prognostic evaluation of assumptions used by cumulus parameterization. Mon Weather Rev 121:764–787. doi:10.1175/1520-0493(1993)121<0764:PEOAUB>2.0.CO;2

Hirakuchi H, Giorgi F (1995) Multilayer present day and $2\times CO_2$ simulations of monsoon climate over eastern Asia and Japan with a regional climate model nested in a general circulation model. J Geophys Res 100:21105–21125. doi:10.1029/95JD01885

Holtslag AAM, de Bruijn EIF, Pan HL (1999) A high resolution air mass transformation model for short range weather forecasting. Mon Weather Rev 118:1561–1575. doi:10.1175/1520-0493(1990)118<1561:AHRAMT>2.0.CO;2

Jones RG, Murphy JM, Noguer M (1995) Simulation of climate change over Europe using a nested regional climate model, I. Assessment of control climate, including sensitivity to location of lateral boundaries. Q J R Meteorol Soc 121:1413–1449

Kalnay E et al (1996) The NMC/NCAR 40-year reanalysis project. Bull Am Meteorol Soc 77:437–471. doi:10.1175/1520-0477(1996)077<0437:TNYRP>2.0.CO;2

Kiehl JT, Hack JJ, Bonan GB, Boville BA, Briegleb BP, Williamson DL, Rasch PJ (1996) Description of the NCAR community climate model (CCM3). NCAR technical note NCAR/TN-420+STR, 152 pp

Koster R, Surez M (1992) Modeling the land surface boundary in climate models as a composite of independent vegetation stands. J Geophys Res 97:2697–2715

Leung RL, Ghan SJ (1995) A subgrid parameterization of orographic precipitation. Theor Appl Climatol 52:95–118. doi:10.1007/BF00865510

Loveland TR, Merchant JW, Ohlen DO, Brown JF (1991) Development of a land cover characteristics database for the conterminous United States. Photogram Eng Remote Sens 57:1453–1463

Marinucci MR, Giorgi F (1992) A $2\times CO_2$ climate change scenario over Europe generated using a limited area model nested in a general circulation model, 1, Present-day seasonal climate simulation. J Geophys Res 97:9989–10009

Mohanty UC, Dimri AP (2004) Location specific prediction of probability of occurrence and quantity of precipitation over Western Himalayas. Weather Forecast 19(3):520–533. doi:10.1175/1520-0434(2004)019<0520:LPOTPO>2.0.CO;2

New MG, Hulme M, Jones PD (2000) Representing twentieth century space time climate variability, Part II: Development of a 1901–96 monthly grids of terrestrial surface climate. J Clim 13:2217–2238. doi:10.1175/1520-0442(2000)013<2217:RTCSTC>2.0.CO;2

Pielke R, Avissar R (1990) Influence of landscape structure on local and regional climate. Landsc Ecol 4:133–155. doi:10.1007/BF00132857

Seth A, Giorgi F, Dickinson RE (1994) Simulating fluxes from heterogeneous land surfaces: explicit subgrid method employing the biosphere–atmosphere transfer scheme (BATS). J Geophys Res 99:18561–18667. doi:10.1029/94JD01330

Sivapalan M, Woods RA (1995) Evaluation of the effects of general circulation model's subgrid variability and patchiness of rainfall and soil moisture on land surface water balance fluxes. In: Kalma JD, Sivapalan M (eds) Scale issues in hydrological modeling. Wiley, New York, pp 453–473

Willmott CJ, Matuura K (2001) Terrestrial air temperature and precipitation monthly and annual time series (1950–1999) (version 1.02). Centre for Climate Research, University of Delware, Newark, NJ, USA. http://climate.geog.udel.edu/~/hjtml-pages/README.ghcn_ts2.html